THE ASTROPHYSICAL JOURNAL, 313:651–661, 1987 February 15

BROAD-BAND PROPERTIES OF THE CfA SEYFERT GALAXIES. I. RADIO PROPERTIES

R. A. EDELSON
Owens Valley Radio Observatory, California Institute of Technology
Received 1986 February 11; accepted 1986 August 14

ABSTRACT

Quasi-simultaneous high-sensitivity observations of a complete, unbiased sample of 42 bright, spectroscopically selected Seyfert galaxies have been made at 1.5, 6, and 20 cm. All of the objects observed were detected above 0.3 mJy at 6 cm. Seyfert 2 galaxies tend to have steep, straight radio spectra with $\langle \alpha_6^{20} \rangle \approx -0.7$. Although this is often true for Seyfert 1 galaxies as well, there is a higher tendency for Seyfert 1 galaxies to have flat spectra, and it appears that $\sim 25\%$ of the Seyfert 1 galaxies have highly curved spectra which flatten out toward higher frequencies. This may be due to emission from a compact core or from the low-frequency side of the infrared power law. There is evidence for extended emission, probably from the disk of the underlying galaxy, in about half of the objects studied. There is no significant difference in the mean 6 cm radio luminosity of types 1 and 2 Seyfert galaxies in this well-defined sample. The radio luminosity of Seyfert galaxies is well correlated with optical luminosity but not with the presence of nearby companion galaxies. Fits to the relation $L_{\rm rad} \propto L_{\rm opt}^s$ yields a value of s significantly steeper than $s = 1$. While most Seyfert galaxies have $\alpha_0^R \approx 0$, the radio and optical-infrared continua apparently originate in different regions. Seyfert galaxies are generally not variable at 20 cm over time scales of ~ 5 yr. There are of order 10^5 Seyfert galaxies Gpc^{-3} with radio luminosities between $10^{36.6}$ and $10^{39.4}$ ergs s^{-1}. There is a sharp cutoff in the radio luminosity function of Seyfert 2 galaxies below $10^{37.2}$ ergs s^{-1}.

Subject headings: galaxies: Seyfert — luminosity function — radio sources: galaxies

I. INTRODUCTION

The radio properties of "radio-quiet" active galactic nuclei (AGNs) are not well understood. The first quasars were discovered because of their radio emission, but only a small fraction of optically selected quasars (and Seyfert galaxies) are "radio-loud" objects (i.e., objects which have much higher flux densities at radio wavelengths than at optical wavelengths; see, e.g., Condon *et al.* 1981*b*). Some models of continuum emission (such as those involving beaming) posit that the intrinsic radio properties of radio-loud sources are the same as those of the underlying population of AGNs, although the observed radio properties are quite different. The radio properties of radio selected sources are well known (i.e., Kühr *et al.* 1981), but these objects tend to be at the extreme radio-loud end of the radio luminosity function, so their behavior is not representative of the underlying distribution of AGNs.

Relatively low detection rates in radio surveys of complete, homogeneous, optically selected samples of Seyfert galaxies and quasars have frustrated attempts to determine the radio properties of the underlying population of AGNs. Meurs and Wilson (1984), in work based partially on a survey by de Bruyn and Wilson (1976), detected $\sim 60\%$ of a sample of Markarian Seyfert galaxies above ~ 4 mJy at 20 cm. These results were incorporated into a 6 cm study by Ulvestad and Wilson (1984*a*), which determined nonsimultaneous spectral indices between 6 and 20 cm for 37% of the original sample of Markarian Seyfert galaxies. A survey of a heterogeneous collection of all active galaxies cataloged before mid 1982 and accessible to the VLA with $V_{\rm rad} \leq 3100$ km s^{-1}, detected all of the objects at 6 cm (Ulvestad and Wilson 1984*b*). However, that sample consists mostly of nearby, low-luminosity objects and is not a complete, unbiased, optically selected sample.

Previous radio surveys of optically selected quasars have also had a low success rate. The similarities in the optical and X-ray properties of optically selected Seyfert 1 galaxies and quasars suggest that their radio properties could also be similar. A 6 cm survey by Condon *et al.* (1981*b*) detected 40% of a heterogeneous sample of optically selected quasars above 0.5 mJy. A quick VLA survey of the PG/BQS quasars detected a similar fraction above 1 mJy at 6 cm (Schaffer *et al.* 1983). A larger fraction are detected in a deep survey (Kellerman 1985), the results of which have not yet been published. The most successful published multifrequency radio survey of optically selected quasars is Condon *et al.* (1981*a*), which determined the radio spectra of 10% of the sources observed.

This paper reports the results of three-frequency observations of the CfA Seyfert galaxies (Huchra and Berg 1987)—a well-defined sample of bright, optically selected Seyfert galaxies. All of the sources observed were detected at 6 cm, and for most, 1.5–20 cm spectra have been determined as well. This permits the radio properties of a well-defined sample of Seyfert galaxies to be probed.

This paper is organized as follows. In the next section, the sample is discussed, and the observations and data are discussed in § III. The radio spectral properties of optically selected Seyfert galaxies are derived and analyzed in § IV. The radio source sizes are discussed in § V, and the relation of radio luminosity to other properties such as optical luminosity and the presence of companion galaxies is investigated in § VI. The Seyfert galaxy radio luminosity function is derived and discussed in § VII, and § VIII contains a concluding discussion and summary of the major results of this paper. Throughout this paper, a value of $H_0 = 75$ km s^{-1} Mpc^{-1} is assumed. Since the largest redshift in this sample is $z = 0.06$, no corrections were made for cosmological effects in the luminosity distance or for evolution.

II. THE CfA SEYFERT GALAXIES

The objects observed were taken from the CfA sample of Seyfert galaxies, a collection of 25 type 1 and 23 type 2 Seyfert galaxies (Huchra and Berg 1987). This sample was derived from the CfA redshift survey (Huchra, Wyatt, and Davis 1982) which obtained spectra of all galaxies with Zwicky magnitudes brighter than $m_{pg} = 14.5$ in a region of sky with $|b| \geq 30°$, $\Omega = 2.66$ sr in extent. The presence of strong emission lines in these spectra was the sole selection criterion used to distinguish these objects from other galaxies in the survey.

For studies of the broad-band properties of Seyfert galaxies, the CfA Seyfert galaxies have a number of advantages over other samples. They are 1–2 magnitudes brighter (and therefore easier to detect at other frequencies) than both the PG/BQS quasars (Schmidt and Green 1983) and the Markarian Seyfert galaxies (Huchra and Sargent 1973). No ultraviolet-excess selection criterion was used in the CfA survey. Selection by ultraviolet excess has been shown to bias samples against strong infrared emitters (Rieke 1978; Edelson, Malkan, and Rieke 1987), and the effect on radio properties is unknown. The Markarian survey is known to be incomplete at both the bright and faint ends (Huchra and Sargent 1973). The results of the V/V_m test performed by Huchra and Berg (1987) indicate that the CfA Seyfert galaxies are distributed uniformly in space, as one would expect from a complete, unbiased sample.

Forty-two of the 48 CfA Seyfert galaxies were observed. Three Seyfert 2 galaxies, NGC 3982, Mrk 461, and IC 4397, were not observed because they were added to the list after the radio measurements were made. Markarian 205 and Mrk 789, both Seyfert 1 galaxies, and NGC 4388, a Seyfert 2, were missed because good optical coordinates were not used. Omission of these six objects from the radio survey is not expected to significantly bias the results, and they will not be discussed further. Intermediate types (i.e., Seyfert 1.5's, etc.) are classified as Seyfert 1 galaxies.

III. OBSERVATIONAL RESULTS

a) Observations

Quasi-simultaneous high-sensitivity measurements of the CfA Seyfert galaxies were made at observing wavelengths $\lambda = 1.5$ cm, 6 cm, and 20 cm. The 1.5 cm measurements were made with the Owens Valley Radio Observatory 40 m telescope, on 1983 July 7–16. The observing system was a beam-switched radiometer using a reflected-wave maser of the NRAO-JPL design (Moore and Clauss 1979), with a cooled Dicke switch. The system temperature was 45 K, with an RF bandwidth of 400 MHz centered on 20.0 GHz (1.5 cm). The FWHM beamwidth was $\sim 1\farcm5$, and the beam separation was $7\farcm1$. Contiguous 40 second scans of each object were combined to form observational records of up to 30 minutes in duration. Each source was observed a number of times during the nine-day run, and the data were combined to yield effective total integration times of a few hours per object. Typical 3 σ upper limits of ~ 2 mJy were obtained for undetected sources. Calibration was done relative to 3C 147, 3C 286, and 3C 295, assuming 1.5 cm flux densities of 1.75 Jy, 2.76 Jy, and 1.07 Jy, respectively (Baars *et al.* 1977).

The measurements at 6 cm and 20 cm were made at the VLA[1] on 1983 July 4. Fifty-megahertz bandwidths were used in the (compact) D-array, and the center frequencies were 4.89 GHz (6 cm) and 1.46 GHz (20 cm). Single snapshots were made of each object with integration times of 10 minutes at 6 cm and of 2.5 minutes at 20 cm. Phase calibrators were observed once every hour. Flux calibration was done relative to 3C 286, which was assumed to have 6 cm and 20 cm flux densities of 14.5 Jy and 7.41 Jy, respectively (Baars *et al.* 1977). Each source was mapped at 6 cm with an untapered synthesized beam of 15″ FWHM (referred to as 6 cm,*h*, hereafter) and with tapered beams of $1\farcm5$ (the size of the OVRO 40 m beam at 1.5 cm) at 6 cm (6 cm,*l*, hereafter) and at 20 cm. The maps were CLEANed with the standard AIPS software. An elliptical Gaussian with its size and orientation matched to those of the synthesized beam was fitted to each map. The position and the amplitude were allowed to vary in the high-resolution 6 cm,*h* map, allowing the right ascension, declination, and central peak flux density to be determined. This position was used and held fixed in fits to the low resolution 6 cm,*l* and 20 cm maps. Only peak low-resolution flux densities were determined from these maps. The 1 σ noise levels for faint and undetected point sources were ~ 0.1 mJy in the high-resolution 6 cm,*h* maps, 0.3 mJy in the low-resolution 6 cm,*l* maps, and 0.5 mJy at 20 cm.

With the exception of one object (0152+06, for which good optical astrometric positions are not available), the 6 cm,*h* sources were required to be within 15″ of published optical astrometric positions. The data of Ledden *et al.* (1980) indicate that the brightest random source expected within 1′ of 0152+06 and 15″ of the 41 remaining optical positions should be weaker than 0.05 mJy. The faintest source detected at 6 cm was brighter than 0.3 mJy, so confusion was not a problem.

b) Data

The observational data are presented in Table 1. The first four columns, which give the name, type (Seyfert 1 or 2), redshift, and integrated optical flux density for each object, are taken from Huchra and Berg (1986). All quoted flux densities are in millijanskies. The optical flux densities are based on Zwicky magnitudes, which represent the sum of nuclear plus galactic light. Since all objects in the sample have $|b| \geq 30°$, no correction is made for Galactic absorption. The positions in columns (5) and (6) were determined with the VLA from the 6 cm,*h* maps and are generally good to 1″. The last four columns contain the flux densities and uncertainties for the 20 cm data ($S_{20\text{ cm}}$), the high-resolution 6 cm data ($S_{6\text{ cm},h}$), the low-resolution 6 cm data ($S_{6\text{ cm},l}$), and the 1.5 cm data ($S_{1.5\text{ cm}}$). The quoted uncertainty is the quadratic sum of the statistical errors and an estimated 5% uncertainty in the calibration. Upper limits are at 3 σ. Of the 42 sources observed, all were detected at 6 cm,*h*, 41 (98%) were detected at 6 cm,*l*, 38 (90%) were detected at 20 cm, and 24 (57%) were detected at 1.5 cm.

Spectral indices are computed and presented in Table 2. The spectral index, α_a^b, is defined as

$$\alpha_a^b = \frac{\log S_a - \log S_b}{\log \nu_a - \log \nu_b} .$$

Columns (1)–(2) are the same as in Table 1. Columns (3)–(4) contain the spectral indices α_6^{20} (defined between 6 cm,*l* and 20 cm), and $\alpha_{1.5}^6$ (from 1.5 cm to 6 cm,*l*), respectively. Column (5) contains the quantity R, defined as

$$R = S_{6\text{ cm},h}/S_{6\text{ cm},l} .$$

Column (6) contains the radio-optical spectral index (α_6^R). This

[1] The National Radio Astronomy Observatory is operated by Associated Universities, Inc., under contract with the National Science Foundation.

TABLE 1

CfA SEYFERT GALAXY RADIO DATA

Source	Type	z	S_{opt} (mJy)	R. A.	Dec.	S_{20cm} (mJy)	$S_{6cm}(h)$ (mJy)	$S_{6cm}(l)$ (mJy)	$S_{1.5cm}$ (mJy)
Mkn 334	2	0.0220	6.9	0 0 35.65	21 40 55.0	26.9 ± 1.4	11.20 ± 0.57	11.4 ± 0.6	4.5 ± 0.7
Mkn 335	1	0.0259	10	0 3 45.26	19 55 29.0	4.1 ± 0.9	3.30 ± 0.18	2.9 ± 0.2	< 1.7
0048+29	1	0.0359	9.1	0 48 53.05	29 7 48.2	7.3 ± 0.5	2.03 ± 0.15	2.8 ± 0.3	< 1.8
I Zw 1	1	0.0604	7.6	0 50 57.84	12 25 19.7	8.4 ± 0.9	2.78 ± 0.17	3.1 ± 0.2	< 1.9
Mkn 993	2	0.0154	10	1 22 42.68	31 52 36.6	3.5 ± 0.5	2.16 ± 0.12	1.9 ± 0.2	< 2.2
Mkn 573	2	0.0173	10	1 41 22.90	2 5 56.5	16.1 ± 1.1	7.08 ± 0.39	7.4 ± 0.4	< 1.8
0152+06	2	0.0174	6.3	1 52 44.65	6 22 2.0	15.0 ± 2.1	9.43 ± 0.48	9.9 ± 0.6	3.7 ± 0.6
Mkn 590	1	0.0263	10	2 12 0.38	− 0 59 57.0	11.2 ± 1.4	5.23 ± 0.29	7.6 ± 0.4	3.6 ± 0.6
NGC 1068	2	0.0037	300	2 40 7.06	− 0 13 30.3	4610 ± 230	1330 ± 68	1800 ± 90	450 ± 34
NGC 1144	2	0.0288	21	2 52 38.84	− 0 23 7.0	146.0 ± 7.3	29.3 ± 1.7	49.4 ± 2.5	13.9 ± 1.3
Mkn 1243	1	0.0353	6.3	9 57 14.04	13 17 0.3	< 4.8	0.37 ± 0.07	< 0.6	< 2.6
NGC 3079	2	0.0037	130	9 58 34.91	55 55 16.0	591 ± 30	145.0 ± 8.4	259 ± 13	84.5 ± 6.5
NGC 3227	2	0.0038	52	10 20 46.73	20 7 6.9	101.0 ± 5.5	27.5 ± 1.4	35.0 ± 1.9	9.2 ± 1.2
NGC 3362	2	0.0227	14	10 42 15.25	6 51 34.7	11.6 ± 0.8	2.54 ± 0.20	4.5 ± 0.3	< 2.3
1058+45	2	0.0191	9.1	10 58 42.41	45 55 21.6	14.5 ± 1.8	3.67 ± 0.20	3.5 ± 0.4	< 2.6
NGC 3516	1	0.0085	48	11 3 23.20	72 50 22.8	15.5 ± 1.1	6.42 ± 0.46	10.6 ± 1.0	5.3 ± 1.0
Mkn 744	1	0.0091	16	11 37 4.78	32 11 12.8	17.5 ± 1.2	5.40 ± 0.30	7.0 ± 0.4	< 2.9
NGC 4051	1	0.0022	200	12 0 36.29	44 48 35.0	40.6 ± 2.4	7.37 ± 0.51	11.6 ± 0.7	7.4 ± 1.1
NGC 4151	1	0.0030	130	12 8 1.04	39 41 2.1	316 ± 16	125.0 ± 6.4	125.0 ± 6.3	39.9 ± 3.4
NGC 4235	1	0.0077	28	12 14 36.80	7 28 8.9	9.5 ± 0.8	4.68 ± 0.28	5.8 ± 0.3	8.1 ± 1.1
Mkn 766	1	0.0128	13	12 15 55.64	30 5 25.9	35.9 ± 1.9	15.80 ± 0.81	15.4 ± 0.8	5.3 ± 0.7
Mkn 231	1	0.0410	9.1	12 54 5.11	57 8 38.5	255 ± 13	270 ± 14	278 ± 13	123 ± 11
NGC 5033	1	0.0030	160	13 11 9.14	36 51 31.3	108.0 ± 5.6	12.90 ± 0.80	39.8 ± 2.0	15.6 ± 1.8
1335+39	2	0.0201	8.3	13 35 28.51	39 24 31.3	< 37.5	1.61 ± 0.11	1.3 ± 0.3	< 1.8
NGC 5252	2	0.0231	6.3	13 35 44.34	4 47 47.2	19.6 ± 1.1	16.20 ± 0.83	18.1 ± 0.9	8.4 ± 1.0
Mkn 266	2	0.0275	9.1	13 36 14.78	48 31 49.0	107.0 ± 6.2	33.4 ± 1.7	43.3 ± 2.2	14.9 ± 1.3
Mkn 270	2	0.0090	7.6	13 39 41.79	67 55 28.0	12.3 ± 0.8	4.92 ± 0.27	5.2 ± 0.4	< 3.7
NGC 5273	1	0.0036	33	13 39 55.31	35 54 20.0	< 2.8	1.59 ± 0.13	2.0 ± 0.3	< 2.4
Mkn 279	1	0.0304	6.3	13 51 53.63	69 33 12.8	22.4 ± 1.4	7.41 ± 0.39	7.3 ± 0.4	< 3.3
NGC 5548	1	0.0166	23	14 15 43.47	25 22 1.9	40.7 ± 2.2	10.50 ± 0.55	13.8 ± 0.9	3.8 ± 0.7
NGC 5674	2	0.0248	13	14 31 22.53	5 40 37.7	28.6 ± 1.7	3.69 ± 0.23	9.6 ± 0.6	2.9 ± 0.8
Mkn 817	1	0.0314	7.6	14 34 57.99	59 0 41.0	10.0 ± 0.9	6.01 ± 0.32	5.2 ± 0.4	< 2.5
Mkn 686	2	0.0122	11	14 35 19.53	36 47 3.2	5.6 ± 0.6	1.71 ± 0.10	2.9 ± 0.5	< 2.1
Mkn 841	1	0.0364	10	15 1 36.20	10 37 55.8	< 14.8	3.89 ± 0.93	6.5 ± 2.1	< 2.2
NGC 5929	2	0.0083	10	15 24 18.95	41 50 41.2	100.0 ± 5.2	20.8 ± 2.5	42.0 ± 2.1	14.3 ± 1.2
NGC 5940	1	0.0339	7.6	15 28 51.25	7 37 37.7	8.5 ± 1.2	2.35 ± 0.17	4.3 ± 0.3	< 1.9
1614+35	1	0.0280	9.1	16 14 40.08	35 49 48.6	9.3 ± 1.1	1.44 ± 0.09	2.8 ± 0.3	< 2.8
2237+07	1	0.0250	7.6	22 37 46.54	7 47 32.8	13.7 ± 1.1	4.63 ± 0.24	4.4 ± 0.4	2.1 ± 0.7
NGC 7469	1	0.0160	23	23 0 44.46	8 36 15.8	171.0 ± 8.9	66.1 ± 3.3	71.4 ± 3.6	22.2 ± 1.9
Mkn 530	1	0.0290	6.9	23 16 22.91	− 0 1 48.1	28.6 ± 1.6	11.50 ± 0.58	11.7 ± 0.6	4.2 ± 0.6
Mkn 533	2	0.0289	14	23 25 24.46	8 30 12.5	220 ± 11	66.5 ± 3.4	75.1 ± 3.8	16.7 ± 1.3
NGC 7682	2	0.0170	7.6	23 26 30.72	3 15 28.0	61.6 ± 3.1	24.6 ± 1.3	24.0 ± 1.2	5.7 ± 0.6

quantity is based on fluxes inferred from Zwicky's integrated galactic photographic magnitudes (with $M = 14.5$ corresponding to $F_\nu = 6.25$ mJy at 4500 Å), and 6 cm,*h* radio measurements. Columns (7)–(8) contain the logarithm of the 6 cm,*h* monochromatic radio luminosity ($L_{\rm rad}$) and monochromatic optical Zwicky galaxy luminosity ($L_{\rm opt}$) in ergs s^{-1}. They are given by

$$L_\nu = 4\pi\nu S_\nu \left(\frac{cz}{H_0}\right)^2 ,$$

where $\nu = 4.89$ GHz and 65 THz for $L_{\rm rad}$ and $L_{\rm opt}$, respectively.

c) *Comparison with Previous Observations*

De Bruyn and Wilson (1976), Meurs and Wilson (1981), and Wilson and Meurs (1982) observed 14 of the objects in this sample with WSRT with a similar beam size at 21 cm from 1975 through 1981. With the exception of one object (Mrk 573), their fluxes are in excellent agreement with those reported here. This indicates that Seyfert galaxies are not generally variable at 20 cm on time scales of ~5 yrs. For Mrk 573, Wilson and Meurs (1981) find a 21 cm flux density of 21.1 ± 1.1 mJy, while Meurs and Wilson (1984) give a flux density of 11.4 mJy. This discrepancy is not explained. A 20 cm flux density of 16.1 ± 0.8 mJy for Mkn 573 is reported here.

Ulvestad and Wilson (1984*a*, *b*) made very high resolution 6 cm observations, with the VLA in the A-configuration, of 13 objects studied in this paper. In general, they found flux densities which were similar to, or slightly less than, the untapered 6 cm,*h* values reported here. This suggests that some objects are extended at 0".5 at 6 cm. The most extreme difference was for Mrk 231, which had a measured 6 cm flux of 170 ± 10 mJy in Ulvestad and Wilson (1984*a*) and 278 ± 14 mJy reported here. Furthermore, Sramek and Tovmassian (1975) report a 6 cm flux density of 137 ± 20 mJy, which differs significantly from both of these results. As the 6 cm,*h* and 6 cm,*l* fluxes are in good agreement for this object, it is probably not extended, but the fact that it is one of the few CfA Seyfert galaxies with a flat spectrum radio source suggests that it may be variable.

IV. RADIO SPECTRA

a) *Low-Frequency Spectra*

Figure 1 contains spectra for the 24 objects which were detected at all three frequencies. Low-frequency spectral indices (α_6^{20}) were determined for the 38 sources (90%) detected

TABLE 2

CfA SEYFERT GALAXY RADIO PARAMETERS

Source	Type	α_{6cm}^{20cm}	$\alpha_{1.5cm}^{6cm}$	R	α_R^O	log(L_{rad}) (erg/s)	log(L_{opt}) (erg/s)
Mkn 334	2	−0.71	−0.66	0.98	−0.036	38.70	43.62
Mkn 335	1	−0.29	...	1.13	0.077	38.32	43.92
0048+29	1	−0.78	...	0.72	0.105	38.39	44.17
I Zw 1	1	−0.82	...	0.89	0.070	38.98	44.54
Mkn 993	2	−0.51	...	1.14	0.107	37.69	43.47
Mkn 573	2	−0.64	...	0.96	0.023	38.30	43.57
0152+06	2	−0.34	−0.70	0.95	−0.030	38.43	43.38
Mkn 590	1	−0.32	−0.53	0.69	0.044	38.53	43.94
NGC 1068	2	−0.78	−0.98	0.74	−0.106	39.23	43.71
NGC 1144	2	−0.90	−0.90	0.59	−0.025	39.36	44.34
Mkn 1243	1	...	...	...	...	37.64	43.99
NGC 3079	2	−0.68	−0.80	0.56	−0.008	38.27	43.35
NGC 3227	2	−0.88	−0.95	0.79	0.044	37.57	42.98
NGC 3362	2	−0.78	...	0.56	0.122	38.09	43.97
1058+45	2	−1.17	...	1.05	0.063	38.10	43.62
NGC 3516	1	−0.31	−0.49	0.61	0.141	37.64	43.64
Mkn 744	1	−0.76	...	0.77	0.075	37.62	43.21
NGC 4051	1	−1.04	−0.32	0.64	0.183	36.52	42.78
NGC 4151	1	−0.77	−0.81	1.00	0.002	38.02	43.17
NGC 4235	1	−0.41	0.24	0.81	0.124	37.41	43.31
Mkn 766	1	−0.70	−0.76	1.03	−0.014	38.38	43.43
Mkn 231	1	0.07	−0.58	0.97	−0.241	40.63	44.28
NGC 5033	1	−0.83	−0.66	0.32	0.176	37.04	43.25
1335+39	2	...	...	1.20	0.115	37.78	43.62
NGC 5252	2	−0.07	−0.54	0.90	−0.068	38.91	43.62
Mkn 266	2	−0.75	−0.76	0.77	−0.093	39.37	43.94
Mkn 270	2	−0.71	...	0.95	0.029	37.57	42.88
NGC 5273	1	...	...	0.80	0.213	36.28	42.73
Mkn 279	1	−0.92	...	1.01	−0.013	38.81	43.86
NGC 5548	1	−0.89	−0.91	0.76	0.054	38.43	43.90
NGC 5674	2	−0.91	−0.85	0.39	0.089	38.33	44.01
Mkn 817	1	−0.53	...	1.15	0.015	38.74	43.97
Mkn 686	2	−0.55	...	0.60	0.130	37.38	43.31
Mkn 841	1	...	...	0.60	0.065	38.68	44.22
NGC 5929	2	−0.72	−0.76	0.50	−0.053	38.13	42.93
NGC 5940	1	−0.57	...	0.55	0.081	38.40	44.04
1614+35	1	−0.99	...	0.51	0.129	38.02	43.95
2237+07	1	−0.94	−0.54	1.05	0.033	38.43	43.77
NGC 7469	1	−0.72	−0.83	0.93	−0.076	39.20	43.86
Mkn 530	1	−0.74	−0.73	0.98	−0.037	38.96	43.86
Mkn 533	2	−0.89	−1.07	0.89	−0.110	39.72	44.18
NGC 7682	2	−0.78	−1.02	1.02	−0.085	38.82	43.44

at 6 and 20 cm. Figure 2 is a histogram of α_6^{20}. The top panel refers to Seyfert 1 galaxies, and the bottom refers to Seyfert 2 galaxies. For Seyfert 1 galaxies, the mean value of α_6^{20} was -0.66, with a dispersion of 0.28 for individual points. For Seyfert 2 galaxies, the mean value of α_6^{20} was -0.71 ± 0.23.

The Kolmogorov-Smirnov (K-S) test, a nonparametric rank test, was used to test for differences between two observed distributions of a parameter (Siegel 1956). The K-S test yields the parameter D, which can be used to determine if the hypothesis that two samples were derived from the same distribution can be rejected at a given confidence level.

Figure 2 suggests that Seyfert 1 galaxies may have a higher tendency to have flat low-frequency radio spectra than Seyfert 2 galaxies. Five Seyfert 1 galaxies (25%) have $\alpha_6^{20} > -0.5$, while only two Seyfert 2 galaxies are this flat. However, because of the small size of this sample, no statistically significant evidence was found with the K-S test for a difference in the distribution of α_6^{20} for types 1 and 2 Seyfert galaxies. A larger sample would be needed to determine the differences, if any, in the distributions of α_6^{20} for different types of Seyfert galaxies.

b) *High-Frequency Spectra and Spectral Curvature*

High-frequency spectral indices ($\alpha_{1.5}^6$) were determined for the 24 sources detected at all three wavelengths. Figure 3 is a plot of α_6^{20} versus $\alpha_{1.5}^6$ for these 24 objects. This quantity appears to be distributed differently for types 1 and 2 Seyfert galaxies. Seyfert 1 galaxies have a mean high-frequency spectral index $\langle\alpha_{1.5}^6\rangle = -0.58 \pm 0.29$ (individual scatter), while for Seyfert 2 galaxies, $\langle\alpha_{1.5}^6\rangle = -0.83 \pm 0.15$. Not only is the mean value of $\alpha_{1.5}^6$ larger for Seyfert 1 galaxies than Seyfert 2 galaxies, but the width of the distribution for Seyfert 1 galaxies is also larger. The results of the K-S test indicates that $\alpha_{1.5}^6$ is distributed differently for types 1 and 2 Seyfert galaxies at the 95% confidence level. The median value of $\alpha_{1.5}^6$ is -0.62 for Seyfert 1 galaxies and -0.82 for Seyfert 2 galaxies. A difference would remain even if NGC 4235, a Seyfert 1 with $\alpha_{1.5}^6 = +0.24$, were excluded from the sample.

Most Seyfert galaxies show little spectral curvature between 1.5 and 20 cm. The quantity $|\alpha_6^{20} - \alpha_{1.5}^6| < 0.25$ for 18 of the 24 objects with measured three-point spectra. Three Seyfert 1 galaxies (NGC 4051, NGC 4235, and 2237+07), but no Seyfert 2 galaxies, have spectra with large upward curvature, $(\alpha_6^{20} - \alpha_{1.5}^6) > 0.40$. This suggests that the spectra of Seyfert 1 galaxies have a tendency to flatten out toward higher frequencies, although the sample is too small for the K-S test to find any statistically significant difference in the distribution of $(\alpha_6^{20} - \alpha_{1.5}^6)$ for type 1 and 2 Seyfert galaxies. Possible explanations are discussed in § IVc. Three sources (Mrk 231, a Seyfert 1 galaxy, and NGC 5252 and 0152+06, both Seyfert 2 galaxies) show strong downward curvature, with $(\alpha_6^{20} - \alpha_{1.5}^6) < -0.35$. All of these sources have flat 6–20 cm spectra, so they are probably becoming optically thick near 6 cm.

c) *Discussion*

Seyfert 2 radio spectral properties are distributed in a similar fashion to those of "normal" optically thin synchrotron sources. They have spectral indices clustered around -0.7 to -0.8, with a small fraction ($\sim 10\%$) having flat radio spectra. They generally show little spectral curvature between 1.5 and 20 cm, and none of the Seyfert 2 galaxies in this sample show extreme spectral flattening toward higher frequencies.

The radio spectral properties of Seyfert 1 galaxies tend to be more broadly distributed than those of Seyfert 2 galaxies, and Seyfert 1 galaxies frequently have radio characteristics not often seen in optically selected radio sources. Seyfert 1 galaxies have flatter high-frequency spectra than Seyfert 2 galaxies ($\sim 20\%$ of the Seyfert 1 galaxies have flat spectra), and $\sim 25\%$ of the Seyfert 1 galaxies in this sample appear to show marked spectral flattening toward high frequencies.

This suggests that the radio emission from Seyfert 2 galaxies is dominated by synchrotron emission from an optically thin source. Most Seyfert 1 galaxies are also dominated by optically thin emission, but something else may be going on in the sources which flatten toward higher frequencies. Two possible explanations are (1) some Seyfert 1 galaxies contain a flat spectrum core not found in Seyfert 2 galaxies, which is becoming visible against the steep spectrum extended emission near 1.5 cm; or (2) in some Seyfert 1 galaxies, low-frequency emission from the nonthermal power-law component, which dominates the optical-infrared continuum of Seyfert 1 galaxies and quasars (but appears to be absent or much weaker in Seyfert 2 galaxies) and which peaks near 100 μm (Edelson and Malkan 1986; Edelson, Malkan, and Rieke 1987), has a flux density which is similar to that of the extended radio emission near 1.5 cm. Millimeter-wave observations could help resolve this issue. The first scenario predicts a flat millimeter spectrum ($\alpha_{mm} \approx 0$), and the second predicts an inverted spectrum ($\alpha_{mm} \geq +1$).

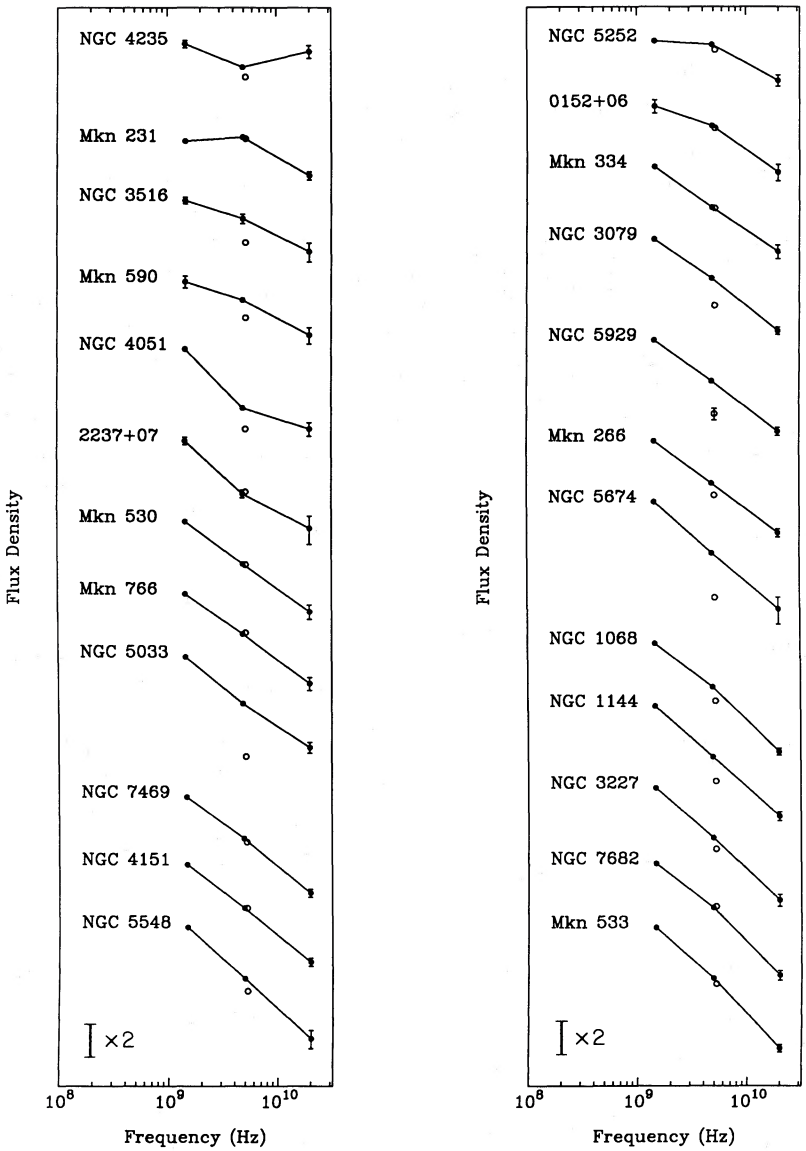

FIG. 1.—Three-point radio spectra (S_ν vs. ν) of the 24 sources detected at all three radio frequencies, *Left*: Seyfert 1 galaxies; *right*: Seyfert 2 galaxies. The two points at 6 cm are the high-resolution data (6 cm,*h*; open circles) and low-resolution data (6 cm,*l*; filled circles). The 6 cm,*h* points have been shifted slightly in frequency to prevent overlap with the 6 cm,*l* points.

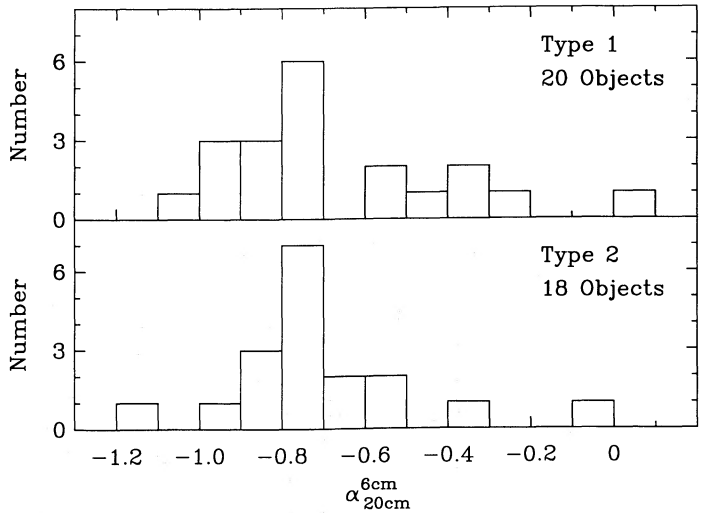

FIG. 2.—Histogram of α_6^{20} for the 38 sources detected at both 6 and 20 cm. *Top*: the data for Seyfert 1 galaxies; *bottom*; data for Seyfert 2 galaxies

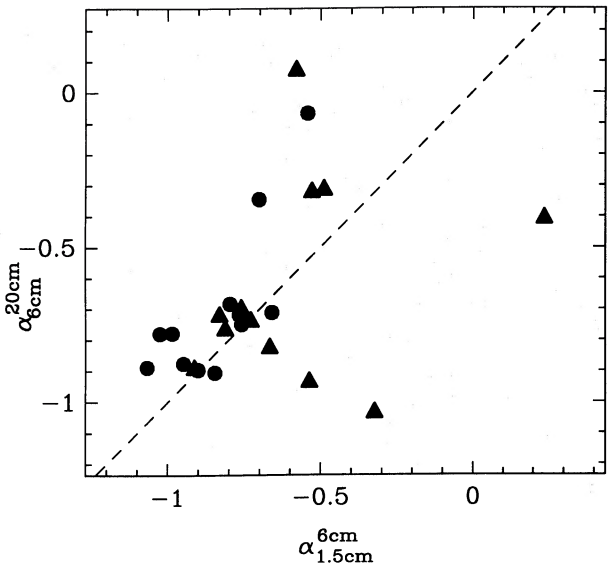

FIG. 3.—Plot of α_6^{20} vs. $\alpha_{1.5}^6$ for the 24 sources detected at all three frequencies. The Seyfert 1 galaxies are denoted by filled triangles, and the Seyfert 2 galaxies by filled circles. A source with $\alpha_6^{20} = \alpha_{1.5}^6$ would lie on the dashed line. Sources with $\alpha_6^{20} < \alpha_{1.5}^6$ (i.e., which flatten toward higher frequency) lie below this line. Errors associated with these spectral indices are generally ~0.07, which is slightly larger than the symbols.

V. RESOLUTION EFFECTS

Untapered 6 cm maps, with a beam width of 15″, and tapered 6 cm maps, with a beam width of 1.′5, were made of the CfA Seyfert galaxies. This corresponds to 4 and 25 kpc, respectively, for an object at a redshift $z = 0.02$ (the median redshift of the sample). Thus, the large beam typically samples the entire galaxy, including the disk, while the small beam contains only the central source. The quantity R, defined as the ratio of the flux in the central beam of the untapered map to that in the tapered map, is a good measure of the degree of resolution at 6 cm. Figure 4 contains a histogram of this quantity, which is tabulated in column (5) of Table 2, for the 41 sources for which R was determined. Statistical fluctuations cause some sources to have values of R greater than unity. In no case is the value of R more than 1.5 σ above unity.

Many of the Seyfert galaxy radio sources are extended at 6 cm. About half (20 of 41) of the sources have $R < 0.8$, and three sources (NGC 5033, NGC 5674, and NGC 5929) have $R < 0.5$. No difference was found in the distribution of R for types 1 and 2 Seyfert galaxies with the K-S test.

This effect is most easily explained as due to emission from the disk of the underlying galaxy. The 21 cm data of Hummel (1981), corrected to 6 cm with a spectral index of −0.7, yields a mean value of $S_{rad}/S_{opt} = 0.4$ for 6 cm disk emission from normal spiral galaxies. The mean value of S_{rad}/S_{opt} is 1.7 for Seyfert galaxies (see § VIc). This suggests that, on average, the disk will contribute about 0.4/1.7 = 24% of the total 6 cm flux (i.e., $\bar{R} = 0.76$), although the ratio should be higher for Seyfert galaxies with low radio luminosities. The observed mean value is $\bar{R} = 0.81$ for the CfA Seyfert galaxies, in good agreement with this expectation.

VI. RELATION TO OTHER PROPERTIES

a) *Radio Luminosity of Seyfert 1 and 2 Galaxies*

The relative luminosity of types 1 and 2 Seyfert radio sources is important for models which relate them in an evolutionary sequence, as well as models of the interaction between radio jets or plasmoids and broad-line-region gas (e.g., Osterbrock 1984). Since all of the objects observed in this complete sample were detected at 6 cm, these data can be used for a rigorous investigation of the radio luminosities of Seyfert galaxies, as well as the relation between radio power and other properties.

Figure 5 is a plot of radio power (L_{rad}) as a function of optical power (L_{opt}). Solving for the mean of the logarithm of the luminosity is equivalent to taking its harmonic mean. For Seyfert 1 galaxies, this mean radio luminosity is $10^{37.98\pm0.90}$ ergs s^{-1} (RMS scatter for individual objects), while for Seyfert 2 galaxies, it is $10^{38.16\pm0.67}$ ergs s^{-1} The median radio luminosity of Seyfert 1 galaxies is $10^{38.14}$ ergs s^{-1} while for Seyfert 2 galaxies, it is $10^{38.05}$ ergs s^{-1}.

No difference was found in the distribution of L_{rad} for types 1 and 2 Seyfert galaxies with the K-S test. While the mean radio

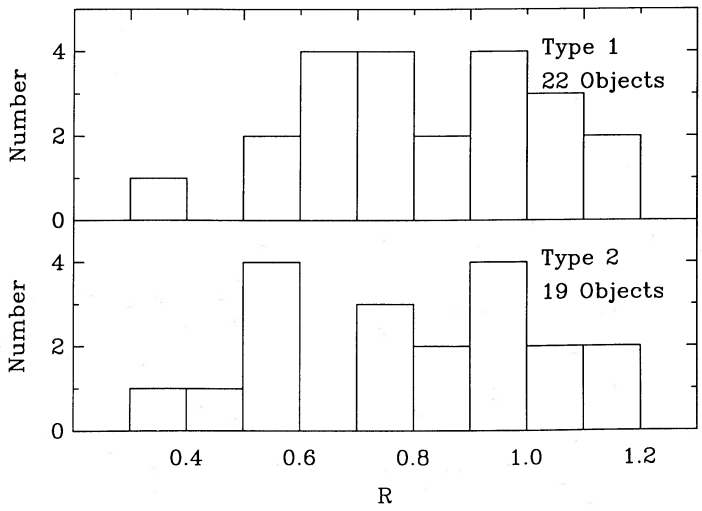

FIG. 4.—Histogram of R, a measure of the degree of resolution of the 6 cm radio source for the 41 sources detected with both 6 cm,*h* and 6 cm,*l* beams. *Top*: the data for Seyfert 1 galaxies; *bottom*; data for Seyfert 2 galaxies.

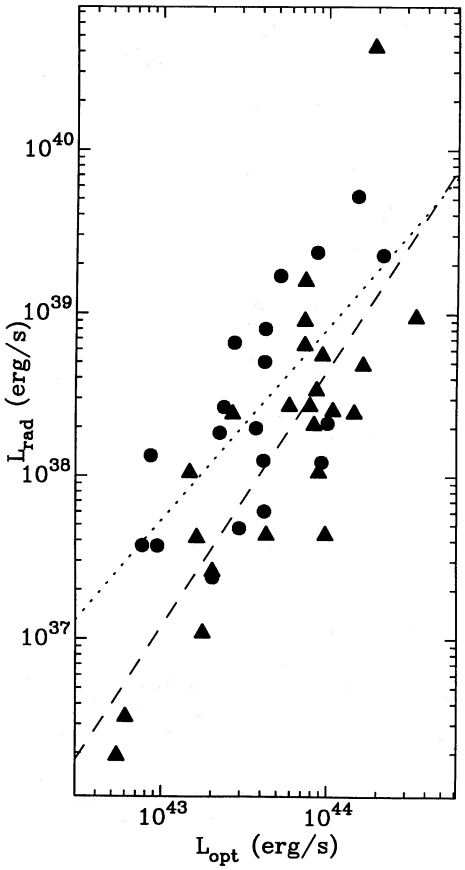

FIG. 5.—Plot of radio luminosity (L_{rad}) as a function of optical luminosity (L_{opt}). Seyfert 1 galaxies are denoted by filled triangles, and Seyfert 2 galaxies by filled circles. The dashed line is a proper least-squares power-law fit for Seyfert 1 galaxies and the dotted line for Seyfert 2 galaxies.

luminosities are clearly not significantly different, Seyfert 1 galaxies appear to have a broader distribution of radio luminosities than Seyfert 2 galaxies. However, this trend is not statistically significant in this small sample.

This result is different than that found by Meurs and Wilson (1984). Based on a higher radio detection rate for Seyfert 2 galaxies in a survey of a heterogeneous sample composed primarily of Seyfert galaxies taken from the Markarian survey, they concluded that Seyfert 2 galaxies are more powerful radio sources that Seyfert 1 galaxies. Selection effects are the most likely cause for this difference. Relative to Seyfert 1 galaxies, the ultraviolet-excess–selected Markarian sample contains half as many Seyfert 2 galaxies as the CfA sample. It primarily missed red, low-luminosity Seyfert 2 galaxies, which were included in the spectroscopic CfA survey (Huchra, Wyatt, and Davis 1982). The strong correlation between optical and radio luminosity causes the Markarian sample to be biased against the inclusion of radio-weak Seyfert 2 galaxies. Furthermore, Seyfert 1 galaxies are more optically luminous (and therefore more distant in magnitude-limited surveys), and the distribution of α_0^R is broader for Seyfert 1 galaxies than for Seyfert 2 galaxies (see § VIc). These effects will all tend to depress the radio detection rate of Seyfert 1 galaxies relative to that of the Seyfert 2 galaxies in their sample.

Figure 5 shows that the intrinsic spread in L_{rad} for both types of Seyfert galaxies is much larger than any difference which there may be in the mean values of L_{rad}. (The same is true for L_{rad}/L_{opt}; see § VIc) Differences in the radio powers of Seyfert galaxies of the same types are at least as great as global differences between different types. Theories which explain the radio luminosities of Seyfert galaxies in terms of confinement of the synchrotron source by broad-line region clouds must take this large spread in L_{rad} into account.

b) *Radio and Optical Luminosity*

All of the objects in this well-defined sample were detected at both radio and optical wavelengths, so it is valid to test for luminosity-luminosity correlations. Figure 5 suggests that there is a strong correlation between L_{rad} and L_{opt} for both types 1 and 2 Seyfert galaxies.

The Spearman Rank Test (see Siegel 1956), a nonparametric rank test, was used to search for correlations between parameters. This test yields t, the student's t-statistic, which is used to determine if the hypothesis that the two variables are uncorrelated can be rejected at a given confidence level. The results of this test indicates that L_{rad} and L_{opt} are correlated for both types of Seyfert galaxies above the 99.9% confidence level.

Proper least-squares fits to the power-law relation $L_{rad} \propto L_{opt}^s$ were made to the data. The final regression line is the mean of two regressions, each of which was done using a different variable as the independent variable. For Seyfert 1 galaxies, $s = 1.95 \pm 0.26$, for Seyfert 2 galaxies, $s = 1.66 \pm 0.30$, and for both types of Seyfert galaxy, $s = 1.81 \pm 0.21$. This steep slope is consistent with the results shown in Figure 7 of Meurs and Wilson (1984), although they found no correlation for Seyfert 1 galaxies, and found only a marginal correlation for Seyfert 2 galaxies, probably because of their relatively low detection rate. It is not immediately obvious why the slopes should be significantly steeper than $L_{rad} \propto L_{opt}$. It may be that the strength of the radio source is related to the nonthermal optical point source and that contamination of the optical flux density with light from the underlying galaxy steepens the L_{rad} versus L_{opt} relation.

c) *Radio-Optical Spectral Index*

Figure 6 is a histogram of α_0^R, the radio-optical spectral index. This quantity, given in column (6) of Table 2, is based on the high-resolution 6 cm data (6 cm,*h*) and the integrated Zwicky magnitudes.

Computing the mean radio-optical spectral index is equivalent to computing the harmonic mean of the radio-optical luminosity ratio. For Seyfert 1 galaxies, $\langle \alpha_0^R \rangle = 0.073$, with a 1 σ scatter of 0.118 for individual objects, and for Seyfert 2 galaxies, $\langle \alpha_0^R \rangle = 0.017 \pm 0.109$.

The difference in $\langle \alpha_0^R \rangle$ for types 1 and 2 Seyfert galaxies is 0.056, which corresponds to Seyfert 2 galaxies being on average a factor of 1.9 brighter than Seyfert 1 galaxies with the same optical brightness. The results of the K-S test indicates that the distribution of α_0^R for types 1 and 2 Seyfert galaxies is different at the 99% confidence level. This is a consequence of the fact that Seyfert 1 galaxies are optically more luminous than Seyfert 2 galaxies, while their radio luminosities are similar.

For all Seyfert galaxies, $\langle \alpha_0^R \rangle = 0.045$, which corresponds to $S_{rad}/S_{opt} = 1.7$. For most Seyfert galaxies, $\alpha_6^{20} \approx -0.7$. Edelson and Malkan (1986) find that the infrared spectral indicies of Seyfert 1 galaxies are clustered around $\alpha_{IR} \approx -1.3$, with most showing a sharp cutoff near 100 μm. Under the best assumption (synchrotron self-absorption), they found that the infrared emission was confined to a region of order a light day in size. Seyfert 2 galaxies and other dusty objects were found to have

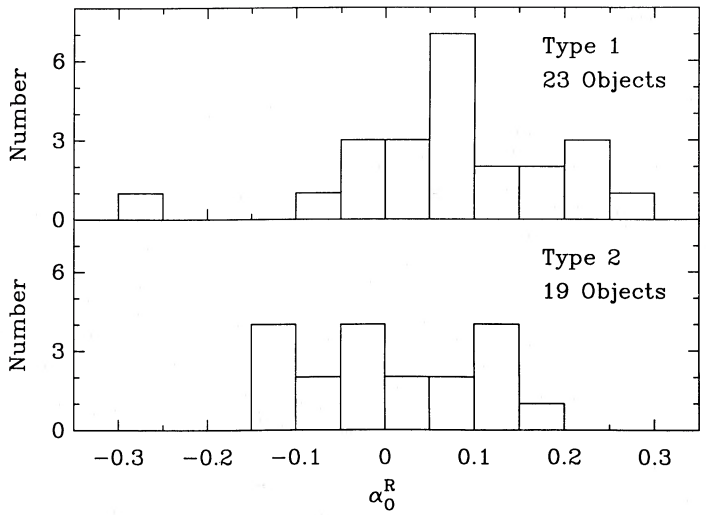

FIG. 6.—Histogram of α_0^R for all 42 sources observed. *Top*: data for Seyfert 1 galaxies; *bottom*: data for Seyfert 2 galaxies. Markarian 231 is the Seyfert 1 with a low value of α_0^R.

even steeper infrared spectra which also peaked in the far-infrared, presumably due to thermal dust emission.

Extrapolation of the far-infrared peak to 6 cm would require a spectral index $\alpha_{100\,\mu m}^{6\,cm} \geq +1$. No sources in this survey have such highly inverted radio spectra. Although this component may be becoming visible in some Seyfert 1 galaxies at 1.5 cm (see § IV), the 6–20 cm spectra of all sources are clearly dominated by more extended emission.

d) Companions

It has been suggested that activity such as radio emission from Seyfert galaxies could be triggered by interactions with other galaxies. Ulvestad and Wilson (1984*a*) found evidence for a correlation between radio emission from Seyfert galaxies and the presence of a companion galaxy, although Ulvestad and Wilson (1984*b*) did not confirm this result. This question is addressed quantitatively in this section.

Two different approaches are used. In the first approach, the CfA redshift survey data (Huchra *et al.* 1983) were used to determine the distance from each of the 14 Seyfert galaxies in this sample with $z \leq 0.015$ (eight type 1 and six type 2 Seyfert galaxies) to its closest companion. The nearest companion was defined to be the galaxy with the smallest angular separation on the sky, provided that galaxy's redshift was no more than 300 km s^{-1} different than that of the Seyfert galaxy and the companion had $m_{pg} \leq 14.5$. No correlation was found between projected distance and radio luminosity with the Spearman rank correlation test.

The second approach used a sample of 28 CfA Seyfert galaxies (15 type 1 and 13 type 2 Seyfert galaxies) for which 6 cm radio data and Dahari's (1985) "interaction parameter" are available. Again, the Spearman rank test was used to test for a correlation between interaction parameter and radio luminosity, but none was found. These results indicate that the radio luminosity of Seyfert galaxies is not a strong function of the presence of companion galaxies.

VII. RADIO LUMINOSITY FUNCTION

a) Introduction

The Seyfert galaxy radio luminosity function (RLF) is an important tool for understanding the nature of Seyfert galaxies and their relation to other objects. If possible, it would be best to determine the Seyfert galaxy RLF from a sample identified in a complete radio survey. Unfortunately, Seyfert galaxies are rather weak radio sources, and they are not found in large numbers in fully identified radio surveys, so this method cannot be used.

The next best method (which is used in this paper) is to make radio measurements of a complete, unbiased, optically selected sample. The RLF is derived from the optical luminosity function and the bivariate radio-optical luminosity distribution function. This method has the disadvantage that errors can be introduced by the spread in L_{rad}/L_{opt}. For instance, no extreme radio-loud objects such as 3C 120 are represented in the CfA Seyfert galaxy sample. Nonetheless, it is used because no other method for determining the Seyfert galaxy RLF is available.

Meurs and Wilson (1984) used this method to determine the RLF of Markarian Seyfert galaxies with 21 cm observations at Westerbork. As the V/V_m test shows that the Markarian survey is incomplete at both the bright and faint ends (Huchra and Sargent 1973), large corrections were applied to the data. However, nothing was done about the bias of the Markarian survey against low-luminosity Seyfert 2 galaxies (see § VI). Non-Markarian Seyfert galaxies were added to the sample, and data were weighted according to the derived value of V/V_m in an attempt to offset the effect of incompleteness. Both the optical luminosity function and the bivariate radio-optical luminosity distribution function were binned. No discussion was made of errors introduced by the double binning process or by the spread in the L_{rad}/L_{opt}. Further assumptions about the distribution of L_{rad}/L_{opt} were required because only 60% of the sources observed were detected.

The CfA Seyfert galaxies form a complete, unbiased sample (Huchra and Berg 1987), so no large corrections for incompleteness are needed. The fact that the entire sample was detected at 6 cm means that few assumptions had to be made concerning the distribution of L_{rad}/L_{opt}.

b) Derivation

The derivation of the CfA Seyfert galaxy RLF is based on the V/V_m method described in Schmidt and Green (1983). The contribution of each object to the luminosity function is

derived individually, and the final luminosity function is the sum of the individual contributions. This method has the advantage that the data are not binned until the last step, so information is not lost in intermediate steps.

The maximum accessible volume (V_m) is the volume of space within which an object could be detected above both survey limits. There are two possible values for V_m, one based on the optical survey limit ($V_{m_{opt}}$), and the other on the radio survey limit ($V_{m_{rad}}$). The accessible volume is the smaller of these two values, that is,

$$V_m = \min (V_{m_{opt}}, V_{m_{rad}}) .$$

This is equivalent to forming the contribution of each object to the RLF from its contribution to the optical luminosity function and the bivariate radio-optical luminosity distribution function.

Once these quantities have been calculated, the RLF is derived and binned. The differential RLF, $\Phi(L_{rad})$, is given by

$$\Phi(L_{rad}) = \frac{4\pi}{\Omega f \Delta L} \sum_{a=1}^{n} \frac{1}{V_{m_a}} ,$$

summed over all n objects with L_{rad} in each bin of width ΔL (Huchra and Sargent 1973). In this equation, Ω is the amount of sky surveyed optically ($\Omega = 2.66$ sr), and f is the fraction of optically selected objects which were observed at radio frequencies ($f = 0.92$ for the Seyfert 1 galaxies, 0.83 for the Seyfert 2 galaxies, and 0.87 for the entire sample of Seyfert galaxies).

The data were binned using logarithmic bins of width $\Delta L = 10^{0.4}$ (corresponding to one "radio magnitude"). The RLF was determined for radio luminosities of $10^{37.0}$–$10^{39.4}$ ergs s^{-1}. No CfA Seyfert galaxy had radio luminosities between $10^{36.6}$ and $10^{37.0}$ ergs s^{-1}, but an upper limit to the space density of Seyfert galaxies with L_{rad} within this range was derived by using a value of $V_m = 7.2 \times 10^{-4}$ Gpc^3, which is appropriate for an object with $L_{rad} = 10^{36.8}$ erg s^{-1} at a survey limit of 0.35 mJy.

It is difficult to estimate the errors in a RLF derived from an optically selected sample. Besides those which arise from statistical fluctuations, errors can also be introduced by the spread in the distribution of L_{rad}/L_{opt} and by biases or incompleteness in the optical Seyfert galaxy selection process. The optical limit is usually the significant one in a survey with sufficient sensitivity to detect all of the sources at radio wavelengths (i.e., $V_{m_{opt}} < V_{m_{rad}}$ for most objects in this sample), so the spread in L_{rad}/L_{opt} gives rise to a spread in $V_m(L_{rad})$.

The differential RLF was derived for types 1 and 2 Seyfert galaxies separately and for both types together. It is presented in Table 3 and Figure 7. Column (1) contains the binned values

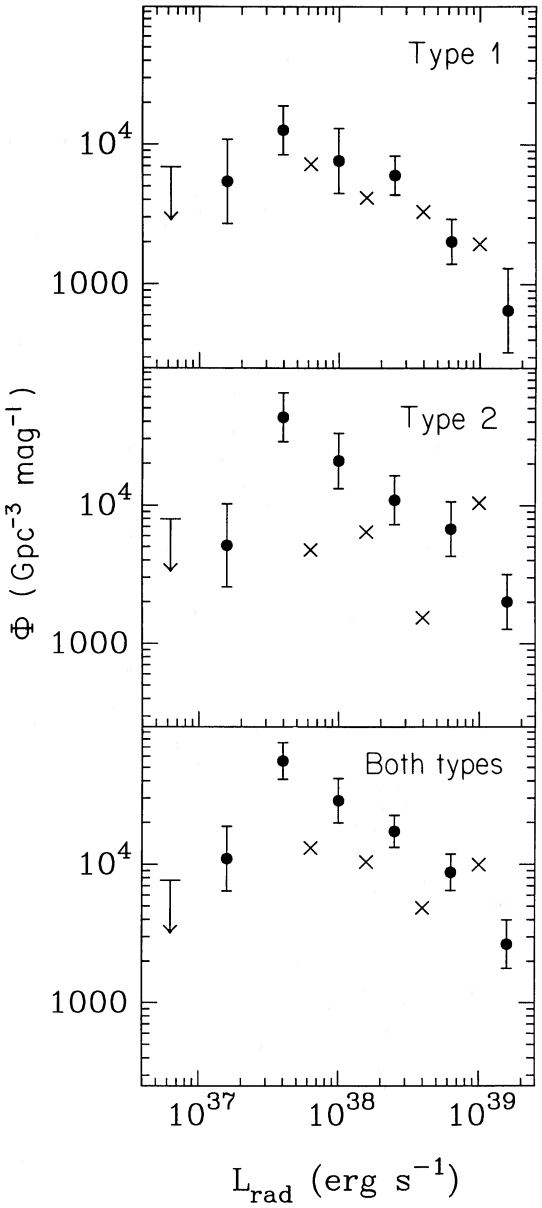

FIG. 7.—The RLF of Seyfert galaxies. Space density is plotted as a function of L_{rad}. (*a*) The RLF of Seyfert 1 galaxies; (*b*) the RLF of Seyfert 2 galaxies, and (*c*) is the RLF of all Seyfert galaxies. Error bars are 1 σ statistical errors. Crosses represent the RLF of Meurs and Wilson (1984).

TABLE 3

SEYFERT GALAXY RADIO LUMINOSITY FUNCTION

	TYPE 1		TYPE 2		BOTH TYPES	
log (L_{rad}) (ergs s^{-1}) (1)	log (Φ) Gpc^{-3} mag^{-1} (2)	N (3)	log (Φ) Gpc^{-3} mag^{-1} (4)	N (5)	log (Φ) Gpc^{-3} mag^{-1} (6)	N (7)
36.6–37.0.....	<3.87	...	<3.90	...	<3.89	...
37.0–37.4.....	3.73	1	3.71	1	4.04	2
37.4–37.8.....	4.10	4	4.63	4	4.75	8
37.8–38.2.....	3.88	2	4.32	3	4.46	5
38.2–38.6.....	3.78	7	4.04	4	4.24	11
38.6–39.0.....	3.30	5	3.83	3	3.94	8
39.0–39.4.....	2.81	1	3.30	3	3.43	4

of L_{rad}. Columns (2)–(3), (4)–(5), and (6)–(7) give the space densities and number of objects in each bin for type 1's, type 2's, and both types together. The error bars in Figure 7 represent the 1 σ statistical uncertainty, uncorrected for the effects discussed earlier. The crosses in Figure 7 represent the RLF of Meurs and Wilson (1984), scaled to the units used in this paper with a 6–20 cm spectral index $\alpha_6^{20} = -0.7$.

c) Discussion

The RLF is determined between $10^{37.0}$ and $10^{39.4}$ ergs s^{-1}, and limits are established for L_{rad} between $10^{36.6}$ and $10^{37.0}$ ergs s^{-1}. The space density of Seyfert galaxies with radio luminosities between $10^{36.6}$ and $10^{39.4}$ ergs s^{-1} is of order 10^5 Gpc^{-3}. All but one of the Seyfert 2 galaxies studied fell within this luminosity range. Markarian 533 had $L_{rad} > 10^{39.4}$ ergs s^{-1}. As is apparent in Figure 5, Seyfert 1 galaxies have a broader range of radio luminosities than Seyfert 2 galaxies (see § V). Two Seyfert 1 galaxies (NGC 4051 and NGC 5273) had $L_{rad} < 10^{36.6}$ ergs s^{-1} and one (Mrk 231) had $L_{rad} > 10^{39.4}$ ergs s^{-1}. For L_{rad} between $10^{36.6}$ and $10^{39.4}$ ergs s^{-1}, Seyfert 2 galaxies are ~ 3 times more numerous than Seyfert 1 galaxies.

There is a dramatic turnover in the RLF of Seyfert 2 galaxies near $10^{37.2}$ ergs s^{-1}. The space density near $10^{37.2}$ ergs s^{-1} is more than one order of magnitude below that extrapolated from higher luminosities. The RLF of Seyfert 1 galaxies also appears to cut off near $10^{37.2}$ ergs s^{-1}, although it is not as strong as that of Seyfert 2 galaxies.

Only four points from the Meurs and Wilson (1984) Seyfert galaxy RLF were of sufficiently low luminosity to overlap the CfA Seyfert galaxy RLF. These points are plotted along with the CfA Seyfert RLF in Figure 7. The RLFs of the Seyfert 1 galaxies are in very good agreement. However, the type 2 Markarian Seyfert galaxy RLF is generally about a factor of 2 below that of the CfA Seyfert galaxies. This suggests that both the Markarian and CfA surveys found most of the Seyfert 1 galaxies, but the Markarian survey missed about half of the Seyfert 2 galaxies, probably because they are too red to satisfy the ultraviolet-excess selection criterion.

VIII. CONCLUSIONS

The results of 1.5, 6, and 20 cm observations of the CfA Seyfert galaxies are reported. The CfA Seyfert galaxies form a complete, spectroscopically selected sample which does not suffer from biases caused by use of the ultraviolet-excess selection technique. It appears that half of the low-luminosity Seyfert 2 galaxies in the CfA Seyfert galaxy sample are too red to be included in the ultraviolet-excess Markarian survey. All of the sources observed were detected at 6 cm. Two-frequency spectra were determined for 90% of these sources, and three-frequency spectra were determined for 57%. The high radio detection rate for this well-defined sample allows the "radio-quiet" end of the Seyfert galaxy radio luminosity function to be probed.

Seyfert 2 radio spectral properties are similar to those of "normal" optically thin synchrotron sources. They have uncurved radio spectra with α_6^{20} clustered around -0.7, and $\sim 10\%$ have flat radio spectra. Most Seyfert 1 galaxies also have steep, uncurved radio spectra, but a larger fraction ($\sim 20\%$) have flat spectra, and about one quarter appear to show strong spectral flattening toward higher frequencies. This could be caused by a second component (either a flat spectrum core or low-frequency emission from the nonthermal component which peaks near 100 μm) becoming visible at 1.5 cm.

Emission from the disk of the underlying galaxy is typically $\sim 20\%$ of the total 6 cm flux density and can be substantially higher for low-luminosity objects. The properties of radio emission from the disks of types 1 and 2 Seyfert galaxies are similar.

There is no significant difference in the radio luminosities of the types 1 and 2 Seyfert galaxies in this complete sample. The intrinsic spread in L_{rad} for either type of Seyfert galaxy is much larger than any differences in the mean radio luminosities. The luminosity of Seyfert galaxy radio sources is strongly correlated with the integrated optical galaxy luminosity. Fits to the power law relation $L_{rad} \propto L_{opt}^s$ yield $s = 1.95 \pm 0.26$ for Seyfert 1 galaxies, $s = 1.66 \pm 0.30$ for Seyfert 2 galaxies, and $s = 1.81 \pm 0.21$ for both types. It is not immediately clear why the slope is significantly steeper than $s = 1$.

In most cases, $\alpha_{IR} \approx -1.3$ and $\alpha_6^{20} \approx -0.7$, while $\alpha_0^R \approx 0$, suggesting that the radio and optical-infrared power-law emission arises from different regions or physical mechanisms. There is no correlation between radio luminosity and the presence of a nearby companion galaxy. Seyfert galaxies are generally not variable on time scales of about 5 years at 20 cm.

There are of order 10^5 Seyfert galaxies Gpc^{-3} with radio luminosities between $10^{36.6}$ and $10^{39.4}$ ergs s^{-1}. Seyfert 2 galaxies are ~ 3 times more numerous than Seyfert 1 galaxies in this luminosity range, but Seyfert 1 galaxies have a broader distribution of radio luminosities. There is a strong cutoff in the RLF of Seyfert 2 galaxies near $L_{rad} = 10^{37}$ ergs s^{-1}, as the derived space density is more than one order of magnitude less than extrapolation from higher luminosities would predict.

The author would like to thank A. Moffet, A. Readhead, M. Schmidt, and L. Dressel for useful and interesting discussions. The anonymous referee made an important contribution to the analysis of the RLF. The assistance of R. Moore and H. Hardebeck of OVRO and J. van Gorkom of the VLA in gathering and analyzing the data is also appreciated. J. Huchra kindly released the list of CfA Seyfert galaxies well ahead of publication. This work was supported by NSF grant AST 85-09822.

REFERENCES

Baars, J. W. H., Genzel, R., Pauliny-Toth, I. K. K., and Witzel, A. 1977, *Astr. Ap.*, **61**, 99.
de Bruyn, A. G., and Wilson, A. S. 1976, *Astr. Ap.*, **53**, 93.
Condon, J. J., Condon, M. A., Jauncey, D. L., Smith, M. G., Turtle, A. J., and Wright, A. E. 1981*a*, *Ap. J.*, **244**, 5.
Condon, J. J., O'Dell, S. L., Puschell, J. J., and Stein, W. A. 1981*b*, *Ap. J.*, **246**, 624.
Dahari, O. 1985, *A.J.*, **90**, 1772.
Edelson, R. A., and Malkan, M. A. 1986, *Ap. J.*, **308**, 59.
Edelson, R. A., Malkan, M. A., and Rieke, G. 1986, *Ap. J.*, submitted.
Huchra, J., and Berg, R. 1987, in preparation.
Huchra, J., and Sargent, W. L. W. 1973, *Ap. J.*, **186**, 433.
Huchra, J. P., Wyatt, W. F., and Davis, M. 1982, *A.J.*, **87**, 1628.
Hummel, E. 1981, *Astr. Ap.*, **93**, 93.
Kellerman, K. I. 1985, private communication.
Kühr, H., Witzel, A., Pauliny-Toth, I. I. K., and Nauber, U. 1981, *Astr. Ap.*, **45**, 367.
Ledden, J. E., Broderick, J. J., Condon, J. J., and Brown, R. L. 1980, *Astr. J.*, **85**, 780.
Meurs, E. J. A., and Wilson, A. S. 1981, *Astr. Ap. Suppl.*, **45**, 99.
———. 1984, *Astr. Ap.*, **139**, 204.
Moore, C. R., and Clauss, R. C. 1979, *IEEE Trans. MTT*, **27**, 249.
Osterbrock, D. E. 1984, *Quart. J.R.A.S.*, **25**, 1.
Rieke, G. H. 1978, *Ap. J.* **226**, 550.

Schaffer, D., Schmidt, M., and Green, R. F. 1983, in *IAU Symposium 97, Extragalactic Radio Sources*, ed. D. S. Heeschen and C. M. Wade (Dordrecht: Reidel), p. 367.
Schmidt, M., and Green, R. F. 1983, *Ap. J.*, **269**, 352.
Siegel, S. 1956, *Nonparametric Statistics for the Behavioral Sciences* (McGraw-Hill).
Sramek, R., and Tovmassian 1975, *Ap. J.*, **196**, 339.
Ulvestad, J. S., and Wilson, A. S. 1984*a*, *Ap. J.*, **278**, 544.
———. 1984*b*, *Ap. J.*, **285**, 439.
Wilson, A. S., and Meurs, E. J. A. 1982, *Astr. Ap. Suppl.*, **50**, 217.

R. A. EDELSON: Owens Valley Radio Observatory, 105-24, California Institute of Technology, Pasadena, CA 91125